

Structural Organization of the Human *Dihydropyrimidine Dehydrogenase* Gene¹

Martin R. Johnson, Kangshang Wang, Silke Tillmanns², Nicolas Albin, and Robert B. Diasio³

Department of Pharmacology and Toxicology, University of Alabama, Birmingham, Alabama 35294

Abstract

Deficiency of the pyrimidine catabolic enzyme, dihydropyrimidine dehydrogenase (DPD), has been shown to be responsible for a pharmacogenetic syndrome in which administration of 5-fluorouracil is associated with severe and potentially life-threatening toxicity. Following the recent availability of the cDNA for DPD, there were initial reports of several molecular defects (point mutations, deletions due to exon skipping) that were suggested as a potential molecular basis for DPD deficiency, even before the complete physical structure of the *DPD* gene was known. To understand the mechanism responsible for DPD deficiency, we have determined the genomic structure and organization of the human *DPD* gene. The gene is approximately 150 kb in length, and it consists of 23 exons, ranging in size from 69 to 1404 bp. The sequences of intronic regions flanking the exon boundaries have been determined. The physical map of the *DPD* gene should permit development of rapid assays to detect point mutations or small deletions in the *DPD* gene associated with 5-fluorouracil toxicity.

Introduction

FUra⁴, synthesized in 1957 and studied extensively by Heidelberger *et al.* (1), today continues to be widely used in the management of several common malignancies, including cancers of the colon, breast, and skin. The anticancer effects and toxicity of FUra are directly related to anabolism of FUra into its nucleotides, which can then produce cytotoxicity through inhibition of thymidylate synthase activity or incorporation into RNA and/or DNA (2).

In humans, more than 85% of administered FUra is degraded through the catabolic pathway (3). DPD (EC 1.3.1.2; also known as dihydrouracil dehydrogenase, dihydrothymine dehydrogenase, and uracil reductase) catalyzes the initial and rate-limiting step in pyrimidine catabolism, the reduction of uracil or thymine to 5,6-dihydrouracil or 5,6-dihydrothymine (4). Thus, DPD regulates the availability of FUra for anabolism, thereby affecting its pharmacokinetics, toxicity, and efficacy (5).

Several recent studies have described a pharmacogenetic disorder in which individuals with absent or significantly decreased DPD activity develop life-threatening toxicity following exposure to FUra (6-10). Administration of standard doses of FUra to DPD-deficient patients has resulted in severe life-threatening toxicity, including mucositis, granulo-cytopenia, neuropathy, and even death. Since the

initial reports several years ago, there have been an increasing number of cases reported suggesting that this disorder may be more frequent than initially thought (7, 11). Population studies in 124 healthy volunteers (7) and 185 cancer patients (11) have demonstrated that approximately 3% of the individuals tested were partially DPD deficient, having enzyme activity below the 95% distribution range of DPD enzyme activity (below 0.064 nmol/min/mg). The recent availability of the *DPD* cDNA (12, 13), has allowed investigators to examine, at the molecular level, patients who were previously phenotyped (by enzyme assay) as DPD deficient. These studies have demonstrated polymorphisms (14) and exon skipping (15, 16) as possible bases for this pharmacogenetic syndrome.

These observations have raised the possibility that there are multiple causes for DPD deficiency. An understanding of the structure and organization of the *DPD* gene should enhance our ability to identify mutations and alternatively spliced regions of this gene. Here, we report the genomic structure and organization for the human *DPD* gene.

Materials and Methods

Library Screening. Clones representing the human genomic locus of the *DPD* gene were isolated from a titrated P1 human genomic library (Genome System Inc., St. Louis, MO). The library was screened using PCR and the following primers: sense, TAGGAAAAGCACTGCAGTACCTTGG, and antisense, CTGGTAGCCAGAATCATTACAGGTCATG. Specific cycling conditions were evaluated prior to screening the P1 library using purified genomic DNA. The conditions used to screen the library were 10 μ M each primer, 60 mM Tris-HCl (pH 8.5), 15 mM (NH₄)₂SO₄, 2.5 mM MgCl₂, 2.5 mM each dNTP, and 1 unit of AmpliTaq DNA polymerase in a total volume of 50 μ l. The samples were amplified in an MJ model PTC-100 thermal cycler (MJ Research, Inc., Watertown, MA) programmed for a temperature-step cycle of 1 min at 95°C, 1 min at 58°C, and 1 min at 72°C. This cycle was repeated for a total of 30 cycles.

Identification of Exon-Intron Boundaries. Approximately 10% of the exon-intron boundaries were identified by direct cycle sequencing (New England Biolabs) of the P1 genomic clone (17) using primers designed from *DPD* cDNA. The remaining boundaries were determined using suppression PCR, as follows (Clontech Laboratories, Inc., Palo Alto, CA). Genomic DNA was digested with *EcoRV*, *ScaI*, *DraI*, *PvuII*, and *SspI* separately. An adaptor was ligated to the ends of the DNA fragments, and a small aliquot of each digested-ligated DNA was used as a template for PCR using adaptor primers and gene-specific primers designed from *DPD* cDNA (18). Amplified products were subcloned into the pCRII vector (Invitrogen) and sequenced using the universal T7 and M13 primers bordering the multiple cloning site. DNA sequencing was accomplished using the dideoxy chain termination procedure (Sequenase Version 2, United States Biochemical Corp.). Exon-intron boundaries were identified by the presence of consensus splice junctions at sites where the sequence of the genomic product differed from the published *DPD* cDNA sequence. The computer programs MacVector and AssemblyLIGN were used for comparison of DNA sequences.

Sizes of introns were determined by exon-exon PCR amplification products using LA PCR (Takara Shuzo Co., Kyoto, Japan) with a buffer supplied by the manufacturer. The final reaction volume was 50 μ l and contained 10 μ M each primer and 50 ng of genomic DNA as a template. Cycling conditions were as follows: denaturation at 98°C for 20 s and annealing and extension at 68°C for 15 min. Following the first 14 cycles, an autosegment extension of 15 s per

Received 1/10/97; accepted 3/26/97.

The costs of publication of this article were defrayed in part by the payment of page charges. This article must therefore be hereby marked *advertisement* in accordance with 18 U.S.C. Section 1734 solely to indicate this fact.

¹ This work was supported by United States Public Health Service Grant CA 62164. N. A. is a recipient of a grant from the National Cancer Institute/European Organization for Research and Treatment of Cancer Exchange Program and the IARC. S. T. was supported by the German-American Fulbright Commission (Commission for Educational Exchange between the United States and Germany).

² Present address: Medizinische Hochschule Hannover, Zentrum Biochemie, Abteilung I Physiologische Chemie, Karl-Wiechert-Allee 9, D-30625 Hannover, Germany.

³ To whom requests for reprints should be addressed, at Department of Pharmacology and Toxicology, Room 101, Volker Hall, University of Alabama, Birmingham, AL 35294. Phone: (205) 934-4578; Fax: (205) 934-8240.

⁴ The abbreviations used are: FUra, 5-fluorouracil; DPD, dihydropyrimidine dehydrogenase; RACE, rapid amplification of cDNA ends.

Table 1 Intron-exon boundaries of the human *DPD* gene

The sequences of the intron-exon boundaries are summarized along with their respective sizes.

Exon	Exon size (bp)	3' intron splice site	Exon sequence (5' to 3')	5' intron splice site	Intron length (bp)
1	140+ ^a	 CATCGAG	gtacggactt	3,554
2	111	ctgtcttttag	AGTATCC. CTGCTTT	gtaagtacca	10,610
3	83	tatgttgcag	AATGTG. CAATGAG	gtaagtctgg	5,055
4	88	tatttcctag	ATGCCTG. AAACAAG	gtaaattcag	12,613
5	166	taatttcgag	AACATAT. TACTGAG	gtaagtata	>20,000
6	193	ttccccgtag	GTATTCA. GTTTAAG	gtaatgccta	7,762
7	82	ttctttttag	TACTTCT. TGTAAG	gtaaatgaaa	5,643
8	88	tttcttatag	ATAATTT. GGAATAG	gtaagtatt	8,414
9	108	tgttacttag	GTTTGCC. AAAGCAG	gtataacata	2,236
10	170	catcattcag	GAATGTG. TGAGGAG	gtaaaatgga	>20,000
11	211	tttgttttag	ATGGAAC. CCTAAG	gtacagtgt	4,610
12	185	gtttttttag	TAAAAGA. CGTACAG	gtaggcattt	5,296
13	216	tattttgcag	TCACAAT. TGATAAG	gtaagaaaa	4,323
14	165	ctttcatcag	GACATTG. AGACAAC	gtaagtgtga	4,972
15	69	ctttttaaag	ATTGTGA. GTCTGAG	gtaatggtta	9,080
16	91	ttgtttaaag	GATTCTG. GATCCAG	gtaaggacct	6,902
17	114	acaggcccag	AGCTGGT. AAGGAAG	gtaagaactt	843
18	121	gtcttgcaag	GTGGTGC. TGTCTGG	gtagggtttg	2,948
19	142	ttttgtgtag	GACAGCA. CCTCCAG	gtcattgtgt	4,011
20	180	tcttttctag	GTATGCA. GGACAAG	gtatgagctt	4,894
21	144	ttccttttag	AAACTGC. CATCAAG	gtaaaaatta	5,107
22	141	ctatttttag	GATGTAA. CTACCAG	gtaagaatcc	2,753
23	1,404	tctgttgcag	GCTATAC		

^a Transcription start site not determined.

cycle (at the annealing and extension step temperature of 68°C) was added for the remaining 16 cycles (19, 20). Most runs included an initial 15-min hold at 94°C and a final 10-min hold at 72°C. All samples were run using a manual "hot start" technique in which Mg²⁺ was withheld until samples had been incubated at 94°C. A positive control that amplified a region of the human β-globin cluster (21.5 kb) was run with each reaction and used the following primers: sense, ACATGATTAGCAAAAAGGGCCTAGCTTGGACTCAGA, and antisense, TGCACCTGCTCTGTGATTATGACTATCCACAGTC.

Primer Extension. Oligonucleotide (CCAGTGACAAACCTCCTT-GCG) was phosphorylated with [γ-³²P]ATP and hybridized to 30 μg of total RNA prepared from freshly isolated peripheral blood mononuclear cells (7). Annealing proceeded in 10 mM Tris-HCl (pH 8.3), 1 mM EDTA, and 250 mM KCl at 60°C for 1 h, followed by incubation at room temperature for 1.5 h. Reverse transcription was performed in 16.7 mM KCl, 13.3 mM MgCl₂, 23.3 mM Tris-HCl (pH 8.3), 13.3 mM DTT, 0.33 mM dNTPs, and 0.133 mg/ml actinomycin D with 200 units of Moloney murine leukemia virus RNaseH⁻ reverse transcriptase (Life Technologies, Inc.). The extension products were fractionated on an 8.0 M urea-6% polyacrylamide gel and analyzed by autoradiography (21).

5'-RACE. Total RNA was prepared from freshly isolated peripheral blood mononuclear cells as described above. 5'-RACE was performed according to the manufacturer's instructions (Clontech). Briefly, cDNA was generated using a modified lock-docking oligo(dT) primer that contained two degenerate nucleotides at the 3' end (22). Second-strand synthesis was performed using a combination of *Escherichia coli* DNA polymerase I, RNase H, and *E. coli* DNA ligase provided by the manufacturer. T4 DNA polymerase was then used to create blunt ends on the double-stranded cDNA. An "adaptor primer" was then ligated to both ends of the double-stranded cDNA using T4 DNA ligase. PCR was then performed using an "anchor primer" complementary to the adaptor primer and a specific DPD cDNA primer located in exon 2. The amplified products were purified, subcloned, and sequenced as described above.

Results and Discussion

In the initial phase of this study, we screened a titrated P1 human genomic library with specific primers (designed within exon 22 of the

DPD DNA sequence). Clones representing the human genomic locus of the *DPD* gene were identified by amplification of a 135-bp product. Three independent P1 clones were isolated, and the boundaries for exons 21–23 were identified by direct thermal cycle sequencing using exon-specific primers. Unfortunately, PCR and hybridization analysis of the three P1 clones demonstrated that they did not contain exons 1–20. The relatively large size of the introns isolated for the *DPD* gene from the P1 screening (23), along with previous reports describing difficulties in screening phage libraries (15), suggested that the average insert size of most commercial λ phage libraries (14–20 kb) would be too small to be useful for this particular gene. We therefore elected to use a recently described technique known as suppression PCR (18, 24, 25). This method had a particular advantage over traditional library screening with regard to the *DPD* gene in that only the boundary of each splice site junction is amplified from genomic DNA and subcloned. Following amplification of each splice site, the PCR products were purified on low melting point agarose and subcloned into the pCRII vector for sequence analysis.

Previous studies have mapped the *DPD* gene to chromosome 1p22 (26). We now report the organization and structure of the *DPD* gene, which consists of 23 exons spanning a region approximately 150 kb in length. The size and sequence of intronic regions flanking the exon boundaries has also been determined and is summarized in Table 1. All intron-exon boundaries were found to conform to the canonical GT-AG rule. A physical map encompassing the entire coding region of the *DPD* gene is shown in Fig. 1. Exons are numbered 1–23, with exon 15 (69 bp) being the smallest and exon 23 (1404 bp) being the largest. The translation start site (ATG) was located in exon 1. Exon 23 contained 168 nucleotides of coding sequence, followed by the translation stop codon (TAA) and a 1236-nucleotide 3' untranslated region. The human liver DPD cDNA sequence published by Yokota *et al.* (12) did not contain the complete 3' untranslated region. Sub-

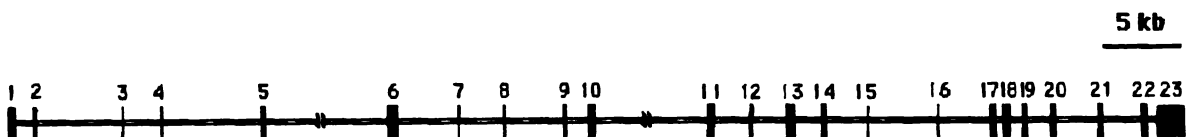


Fig. 1. Organization of the *DPD* gene. Schematic map of the human *DPD* gene; ■, exons 1–23. The initiating ATG is located in exon 1, and the stop codon (TAA) is located in exon 23.

sequent studies in our laboratory identified the complete human lymphocytic *DPD* cDNA sequence (GenBank accession no. U20938), which contained this region and was used in our comparison of genomic and cDNA sequence searching for consensus splice junctions where the sequence of the genomic product differed from the lymphocytic *DPD* cDNA sequence.

Primer extension experiments were undertaken to determine the precise size of exon 1. Freshly isolated RNA from peripheral blood mononuclear cells was used for this analysis. The band indicated by the arrow (Fig. 2) is the reverse-transcribed product, whereas the other bands represent known DNA sequences that were included for determination of molecular size. Comparison of the nucleotides in the known sequence with the mobility of the *DPD* mRNA lane demonstrates that the distance from the primer to the 5' end of the message coding for *DPD* is 104 nucleotides. This result suggested that there were approximately 20–25 additional nucleotides in the mRNA sequence that had not been identified previously by cDNA cloning (12, 13). We used 5'-RACE to clone and sequence these additional nucleotides located upstream from the published *DPD* cDNA sequence. PCR with an anchor primer and an internally nested primer located 193 bp from the 5' end of the published human *DPD* cDNA sequence resulted in the amplification of a cDNA approximately 214 bp in length. Following subcloning, 10 clones were selected and sequenced. All of the inserts examined contained the human *DPD* cDNA sequence reported previously; however, 8 of the 10 clones extended further upstream for an additional 21 nucleotides. These data suggest that exon 1 is 140 nucleotides long and contains 101 nucleotides of 5'

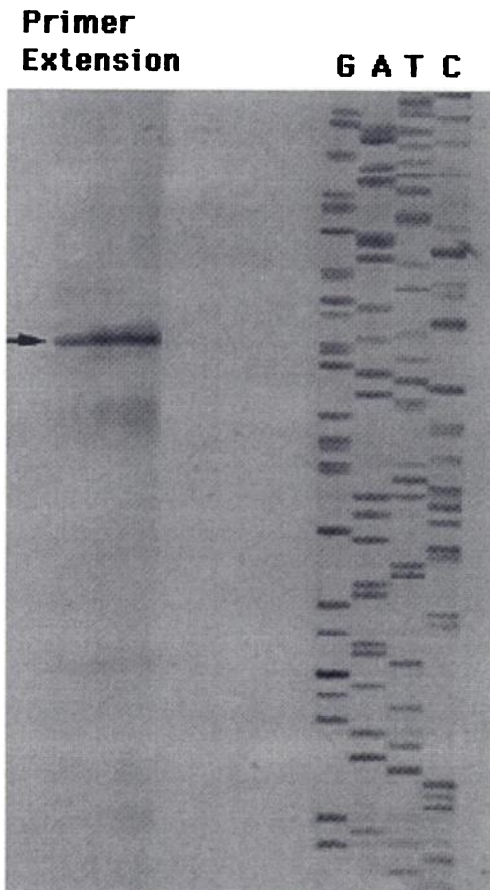


Fig. 2. Determination of the size of exon 1 by primer extension. Primer extension was performed as described in "Materials and Methods." One major (arrow) product was detected.

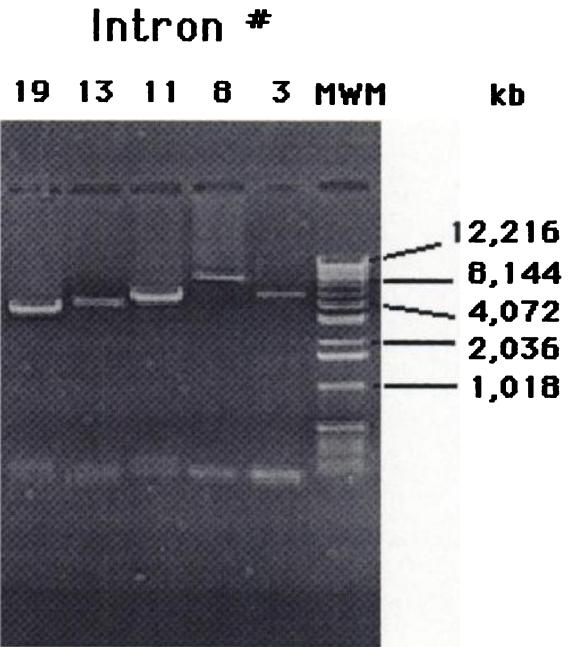


Fig. 3. Sizing of introns for the human *DPD* gene. Sizes of introns were determined by exon-exon PCR amplification products, using either the P1 clone or genomic DNA as the template. PCR products for Introns 19, 13, 11, 8, and 3 are shown (from left to right), resolved on a 1% agarose gel.

untranslated region, followed by the initiating methionine and 36 nucleotides of coding sequence.

Intron sizes were determined by PCR amplification using genomic DNA as a template with gene-specific primer pairs from adjacent exons. The use of nested PCR allowed verification of the sizes of the introns. Only PCRs that gave a single well-defined product (Fig. 3) were used for estimation of intron sizes. Introns 5 and 10 were the largest, with sizes greater than 20 kb, whereas introns 9 and 17 were the smallest.

The recent examination of two unrelated *DPD*-deficient patients has suggested exon skipping (15, 16) as a possible mechanism for *DPD* deficiency. These studies demonstrated a 165-bp deletion in the mRNA of both patients. Genomic DNA analysis of these patients revealed a G to A mutation in the GT 5' splicing recognition sequence of the intron preceding the mutation. It is now clear from the current study that exon 14 represents the skipped exon and that the G to A point mutation in the invariant GT splice donor site is located at the 5' end of intron 14. However, our examination of this region of the *DPD* gene in two additional well-characterized *DPD*-deficient patients has demonstrated that neither patient exhibits this particular G to A mutation⁵.

The aim of this study was to determine the structure and organization of the *DPD* gene. These data could then be used as a foundation for rapidly scanning the *DPD* gene for mutations in genomic DNAs in an attempt to define the molecular basis of *DPD* enzyme deficiency. The data presented in this study should allow the development of genetic assays that could clarify the role of the *DPD* gene in deficient patients. The clinical diagnosis of *DPD* deficiency is difficult because the appearance of life-threatening toxicity secondary to exposure to FUra is the first symptom of this pharmacogenetic syndrome. Until now, only phenotypic *DPD* enzyme assays have been available to diagnose patients as *DPD* deficient. These assays are expensive and labor intensive and are not available in most cancer treatment centers. Thus, there is a great need for a more direct diagnostic method,

⁵ Unpublished work.

preferably available to the patient prior to receiving FUra. The characterization of the genomic structure of the *DPD* gene provides the basis for the development of simple genetic tests. To date, all *DPD*-deficient patients have been analyzed without a complete understanding of the *DPD* gene structure and organization. The stability of DNA in comparison to RNA along with the ease with which DNA samples may be extracted and purified represents a clear diagnostic advantage. In addition, the development of genomic DNA based assays would allow analysis of archive paraffin-embedded samples from deceased *DPD*-deficient patients. These samples would allow researchers to build pedigrees on families (including determination of heterozygotes), who, until now, were impossible to study. Although the size and complexity of the *DPD* gene makes scanning the gene for mutations a challenge, we believe that recent advances in the field of molecular biology (such as single-stranded conformational polymorphism) may be used for identifying additional mutations in the *DPD* gene.

References

- Heidelberger, C. In: A. C. Sartorelli and D. G. John (eds.), *Antineoplastic and Immunosuppressive Agents, Part II*, pp. 193–231. Berlin: Springer-Verlag, 1975.
- Grem, J. L. In: B. A. Chabner and D. L. Longo (eds.), *Cancer Chemotherapy and Biotherapy, Ed. 2*, pp. 149–197. Philadelphia: Lippincott-Raven, 1996.
- Heggie, G. C., Sommadossi, J. P., Cross, D. S., Huster, W. J., and Diasio, R. B. Clinical pharmacokinetics of 5-fluorouracil and its metabolites in plasma, urine, and bile. *Cancer Res.*, 47: 2203–2206, 1987.
- Sommadosi, J. P., Gewirtz, D. A., Diasio, R. B., Aubert, C., Cano, J. P., and Goldman, I. D. Rapid catabolism of 5-fluorouracil in freshly isolated rat hepatocytes as analyzed by high performance liquid chromatography. *J. Biol. Chem.*, 257: 8171–8176, 1982.
- Diasio, R. B., and Lu, Z.-H. Dihydropyrimidine dehydrogenase activity and fluorouracil chemotherapy. *J. Clin. Oncol.*, 12: 2239–2242, 1994.
- Diasio, R. B., Beavers, T. L., and Carpenter, J. T. Familial deficiency of dihydropyrimidine dehydrogenase. *J. Clin. Invest.*, 81: 47–51, 1988.
- Lu, Z., Zhang, R., and Diasio, R. B. Dihydropyrimidine dehydrogenase activity in human peripheral blood mononuclear cells and liver: population characteristics, newly identified deficient patients and clinical implication in 5-fluorouracil chemotherapy. *Cancer Res.*, 53: 5433–5438, 1993.
- Harris, B. E., Carpenter, J. T., and Diasio, R. B. Severe 5-fluorouracil toxicity secondary to dihydropyrimidine dehydrogenase deficiency: a potentially more common pharmacogenetic syndrome. *Cancer (Phila.)*, 68: 499–501, 1991.
- Etienne, M. C., Lagrange, J. L., Dassonville, O., Fleming, R., Thyss, A., Renee, N., Schneider, M., Demard, F., and Milano, G. Population study of dihydropyrimidine dehydrogenase in cancer patients. *J. Clin. Oncol.*, 12: 2248–2253, 1994.
- Takimoto, C. H., Lu, Z. H., Zhang, R., Liang, M. D., Larson, L. V., Cantilena, L. R., Grem, J. L., Allegra, C. J., Diasio, R. B., and Chu, E. Severe neurotoxicity following 5-fluorouracil-based chemotherapy in a patient with dihydropyrimidine dehydrogenase deficiency. *Clin. Cancer Res.*, 2: 477–481, 1996.
- Milano, G., and Etienne, M. C. Potential importance of dihydropyrimidine dehydrogenase (*DPD*) in cancer chemotherapy. *Pharmacogenetics*, 4: 301–306, 1994.
- Yokota, H., Fernandez-Salguero, P., Furuya, H., Lin, K., McBride, O. W., Podschun, B., Schnackerz, K. D., Gonzales, F. J. cDNA cloning and chromosome mapping of human dihydropyrimidine dehydrogenase, an enzyme associated with 5-fluorouracil toxicity and congenital thymine uraciluria. *J. Biol. Chem.*, 269: 23192–23196, 1994.
- Johnson, M. R., Albin, N., Wang, K., and Diasio, R. B. cDNA cloning of dihydropyrimidine dehydrogenase from human lymphocytes. *Proc. Am. Assoc. Cancer Res.*, 36: 503, 1995.
- Albin, N., Johnson, M. R., Shahinian, H., Wang, K., and Diasio, R. B. Initial characterization of the molecular defect in human dihydropyrimidine dehydrogenase deficiency. *Proc. Am. Assoc. Cancer Res.*, 36: 211, 1995.
- Meisma, R., Salguero, P. F., Van Kuilenburg, A. B. P., Van Gennip, A. H., and Gonzalez, F. J. Human polymorphism in drug metabolism: mutation in the dihydropyrimidine dehydrogenase gene results in exon skipping and thymine uraciluria. *DNA Cell Biol.*, 14: 1–6, 1995.
- Wei, X., McLeod, H. D., McMurrough, J., Gonzalez, F. J., and Salguero, P. F. Molecular basis of the human dihydropyrimidine dehydrogenase deficiency and 5-fluorouracil toxicity. *J. Clin. Invest.*, 98: 610–615, 1996.
- Pierce, J. C., Sternber, N., and Sauer, B. A mouse genomic library in the bacteriophage P1 cloning system: organization and characterization. *Mamm. Genome*, 3: 550–558, 1992.
- Siebert, P. D., Chenchik, A., Kellogg, D. E., Lukyanov, K. A., and Lukyanov, S. A. An improved PCR method for walking in uncloned genomic DNA. *Nucleic Acids Res.*, 23: 1087–1088, 1995.
- Barnes, W. M. PCR amplification of up to 35-kb DNA with high fidelity and high yield from λ bacteriophage templates. *Proc. Natl. Acad. Sci. USA*, 91: 2216–2220, 1994.
- Cheng, S., Fockler, C., Barnes, W. M., and Higuchi, R. Effective amplification of long targets from cloned inserts and human genomic DNA. *Proc. Natl. Acad. Sci. USA*, 91: 5695–5699, 1994.
- MacKnight, S. L., and Kingsbury, R. Transcriptional control signals of a eukaryotic protein-coding gene. *Science (Washington DC)*, 217: 316–324, 1982.
- Borson, N. D., Sato, W. L., and Drewes, L. R. A lock-docking oligo(dT) primer for 5' and 3' RACE PCR. *PCR Methods Appl.*, 2: 144–148, 1992.
- Ogata, H., Fujibuchi, W., and Kanehisa, M. The size differences among mammalian introns are due to the accumulation of small deletions. *FEBS Lett.*, 390: 99–103, 1996.
- Maiti, S., Doskow, J., Li, S., Nhim, R. P., Lindsey, J. S., and Wilkinson, M. F. The *Pem* homeobox gene. Androgen-dependent and -independent promoters and tissue-specific alternative RNA splicing. *J. Biol. Chem.*, 271: 17536–17546, 1996.
- Johansson, M., and Karlsson, A. Cloning and expression of human deoxyguanosine kinase cDNA. *Proc. Natl. Acad. Sci. USA*, 93: 7258–7262, 1996.
- Fernandez-Salguero, P., Kimura, S., Gonzalez, F. J., and Yamada, K. Assignment of the human dihydropyrimidine dehydrogenase gene (*DPYD*) to chromosome region 1p22 by fluorescence *in situ* hybridization. *Genomics*, 24: 613–614, 1994.